Limits of the SIE and the thermal analysis on impurity effect evaluation

Kazuaki Yamazawa, Januarius Widiatmo, Jun Tamba and Masaru Arai
National Metrology Institute of Japan, AIST (NMIJ, AIST)

Introduction

Impurities in metal fixed-points cause significant bias to the fixed-point temperature. After a long discussion, CCT-WG1 has recommended methodologies to estimate the uncertainty and to correct the fixed-point temperature for the influence of chemical impurities. At present, it is widely recognized that the SIE (sum of individual estimates) is able to correct the temperature bias. However, the uncertainty of this correction depends on the uncertainty of the chemical analysis and the slope of the liquidus curve. CCT-WG1 is currently surveying the reliability and the uncertainty of these values.

In our recent work at NMIJ, AIST, we have challenged to compare the results from SIE and the thermal analysis of the freezing curves. This challenge includes, improvement of the metal filling method of the fixed point crucibles, enabling the sampling of the metal for both pre-fabrication and post-fabrication, and the development of fixed point furnaces that enable an accurate evaluation of the $1/F$ (F is the liquid fraction).

This paper discusses the application limits of both the SIE and the thermal analysis of the freezing curves as the methods to evaluate the influences of impurities within the fixed point cells, by summarizing the key points of our recent activities.

1. Discussion upon the thermal analysis of the freezing plateaus

In the CCT document CCT/05-08 [1] written by the CCT-WG1, the SIE (sum of individual estimates) is classified to have ability to correct the temperature bias caused by chemical impurities. The document also classifies that thermal analysis, such as the evaluation of the freezing curves or $1/F$ analysis as methods for validation. The agreed state-of-art procedure for treating the observed freezing curve is to adopt the maximum value as the best approximation[1,2]. This agreement might be somewhat due to the definite fact that methods employing the thermal analysis are significantly sensitive and dependant to the experimental apparatus.

The authors well understand this state-of-art, however, we had some inspiration that if a fixed-point apparatus and a realization method enabling an accurate determination of the F can be developed, an evaluation using experimental data and the related theory could also be conducted accurately. We have made the challenge to our inspiration through the improvement stated as follows.

1.1. Improvement of the metal filling method

Most of the high purity metals found in the market are in form of shots. This form is problematic due to its large surface area when considering contamination. The large surface area compared to the volume could easily attract impurities. Difficulties may occur in the filling of the metal crucibles.

NMIJ, with cooperation with Nikko Mining & Metals Co., has solved this problem by introducing a cylinder ingot (32 mm diameter, 200 mm high) for filling the crucible. Figure 1 shows the filling method that reduces the risk of contamination during the filling[3]. Adopting this method, NMIJ has produced the fixed-point cells from In up to Cu, and the analyses results as well as the experimental data on the Al [3,4], Sn [5], Ag [6] points have been published.

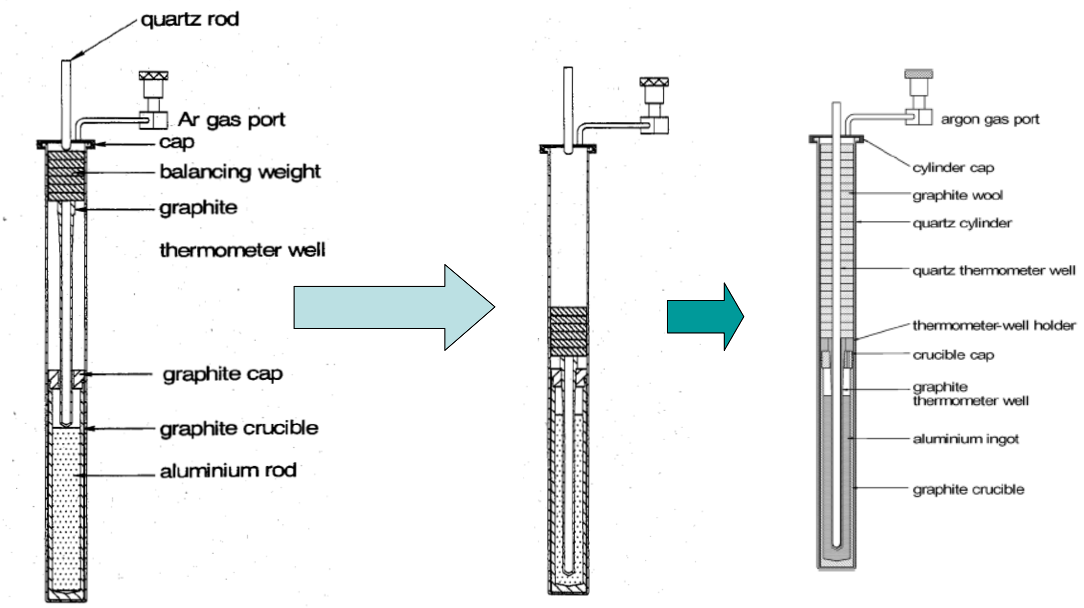

Figure 1 Metal filling method to that reduces the risk of contamination during the filling[3].

1.2. Specimen sampling for the metal in the crucible

Regarding the cell recently fabricated, we have obtained the chemical analyses results for our fixed-point metals, which are analyzed prior cell fabrication. Most of them employ the GDMS (Gas Discharge Mass Spectroscopy), enabling us to apply the SIE method to calculate the temperature bias caused by the detected impurities. For the most recent cells, we have also made an innovation of the cell filing method, that enables the sampling from a funnel used in the filling procedure that we believe that well represents the actual metal filled inside the crucible [6]. Figure 2 shows the method to obtain this post-fabrication sample of the fixed-point metal.

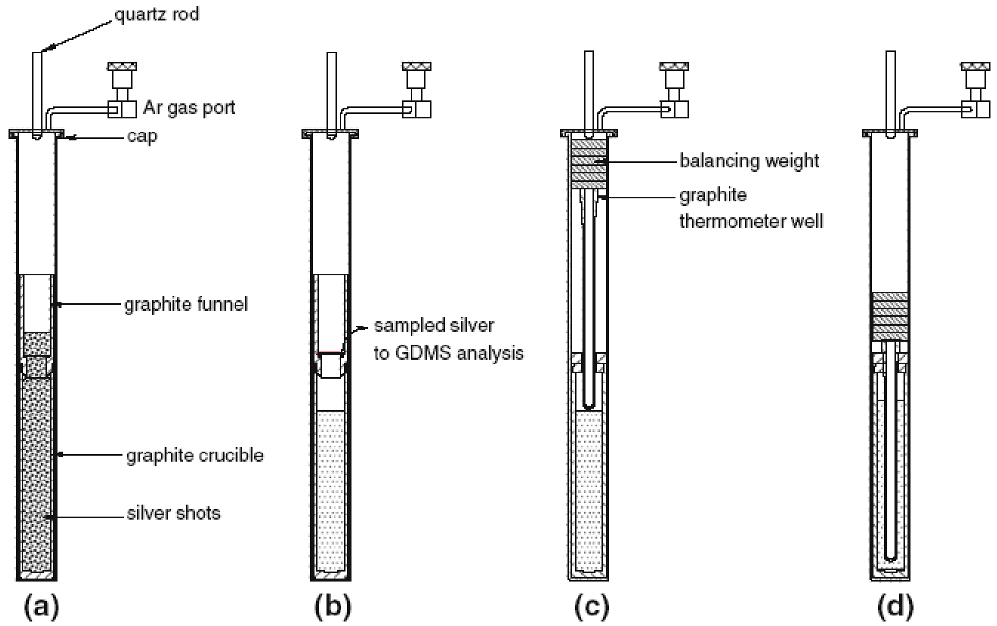

Figure 2 Filling method that enables the post-fabrication sample of the fixed-point metal [6].

1.3. Improvement of the fixed-point furnace for the accurate determination of the 1/F

There are a number of criticisms of the thermal analysis of the melting or freezing plateau. It is difficult to determine accurately the liquid fraction in solid–liquid equilibrium by relying only on the measured temperature. For example, the melt-off point, where the metal has completely melted, may be difficult to determine because the run-off point, where overheated liquid contacts the thermometer well, masks the true liquidus. During solidification, the solid fraction nucleated following supercooling of the liquid metal is likewise difficult to determine. As phase diagrams show that each individual impurity might either raise or depress the liquidus temperature, the observed temperature during the plateau is a sum of a combined phenomenon; merely observing the temperature profile is losing information. For such reasons, it is generally said that an evaluation based on $1/F$ (F is the liquid fraction) analysis of melting or freezing plateau is unreliable.

Another criticism against the conventional realization method employing usual fixed-point furnaces is the existence of heat flux flow during the phase transition. Research using adiabatic calorimetry is commonly used as an alternative.

NMIJ has attempted a challenge against this state-of-art.

We have found in the literature that in many cases regarding the thermal analysis of the freezing plateau using conventional furnaces, the liquid fraction F is determined by a rather systematic method that might misinterpret the value of F. Upon this concern, we have developed fixed point furnaces in new design that basically employs the conventional method, however, having the ability to accurately determine the liquid fraction F.

Figure 3 shows an experimental result at the Sn fixed point employing such a furnace 5). The liquid fraction F can be accurately determined by the observation of the heater power. The heater power fluctuates during the phase transition, and its time integral (energy) well agrees with the total heat of fusion of the metal ingot. Examples of the freezing curves plotted against the 1/F are shown in figure 3. The $1/F$ is determined from the profile of the heater power simultaneously observed during the plateau. As shown in figure 3(a) (6N purity Sn ingot) and 3(b) (5N purity Sn ingot), the freezing plateau plotted against the $1/F$ determined by our method shows a clear linear profile. This linearity is the proof of our high ability of both the fixed-point realization and the evaluation method of the freezing curves.

Such work are also done in the other fixed points, such as Al 3,4) and Ag 6), and for the In and Zn points are expected to be reported in the near future.

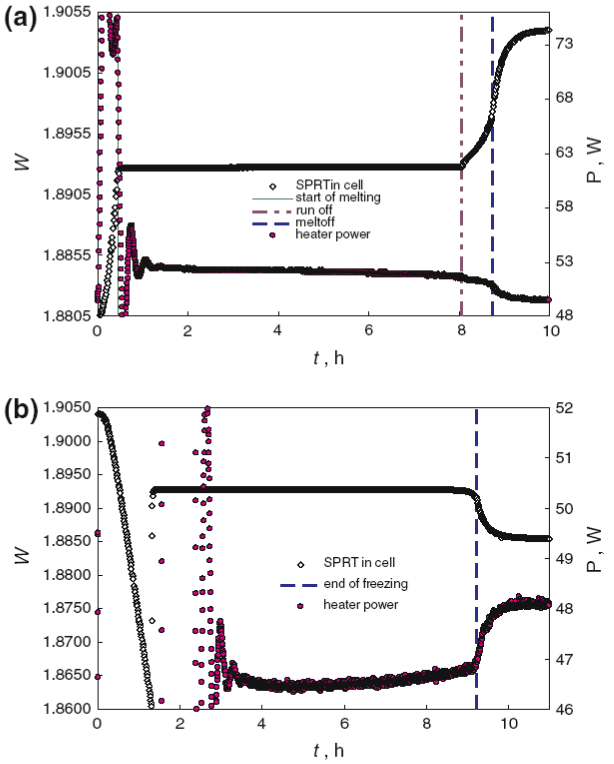

Figure 3 Relation of the melting/freezing plateau to the heater power: (a) during the melting plateau and (b) during the freezing plateau [5)].

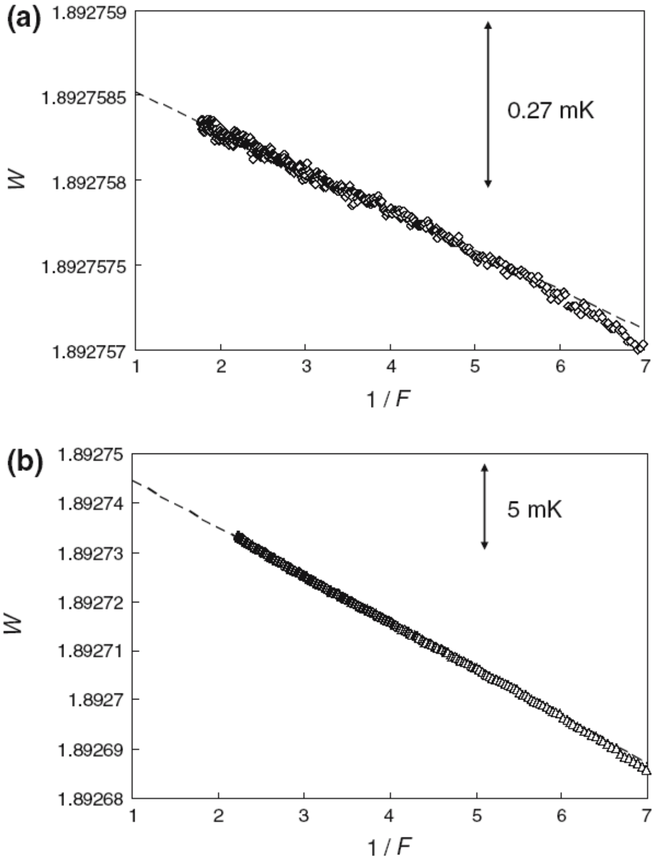

Figure 4 Freezing curve at the tin fixed-point: (a) cell Sn No. 4 and (b) cell Sn No. 6 [5)].

1.4. Comparison with the SIE and the freezing curve analyses

Since we have the chemical analyses for each metal ingot for our newly fabricated cells, we can compare the results of the SIE and the evaluation of the freezing curves. In most of the cells, the results obtained by the SIE, and those obtained from our freezing curve evaluation method, have agreed within their uncertainties.

Figures 5, 6, and 7 show the examples for Al, Sn and Ag.

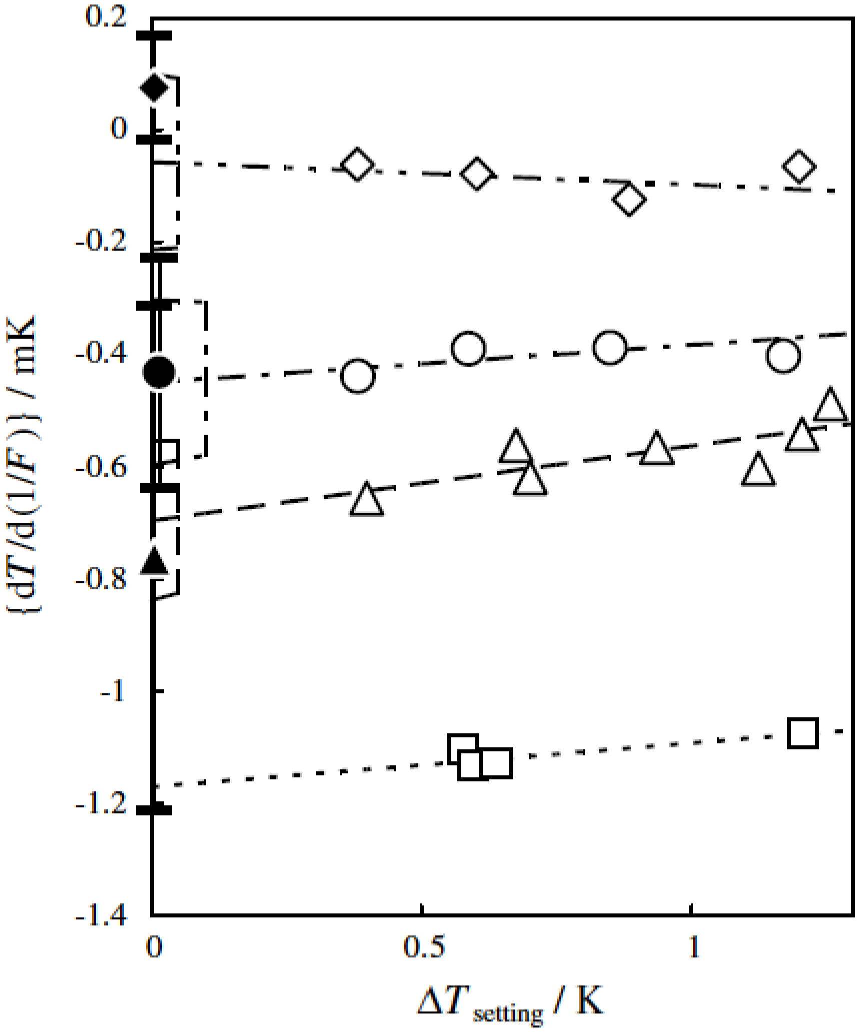

NRLM Al 97-1 (□); Al No 4 (△ and ▲), Al No 5 (○ and ●) and Al No 6 (◇ and ◆).

Figure 5 Comparison between the SIE and the slope of the freezing curve obtained from experimental results for Al cells [4)]. The DT_{SIE} and its uncertainty is indicated as the bold plots, and the experimental results are shown in the open plots. The dotted lines show the trend for the slope of the freezing curve against the temperature setting, which is negligibly small.

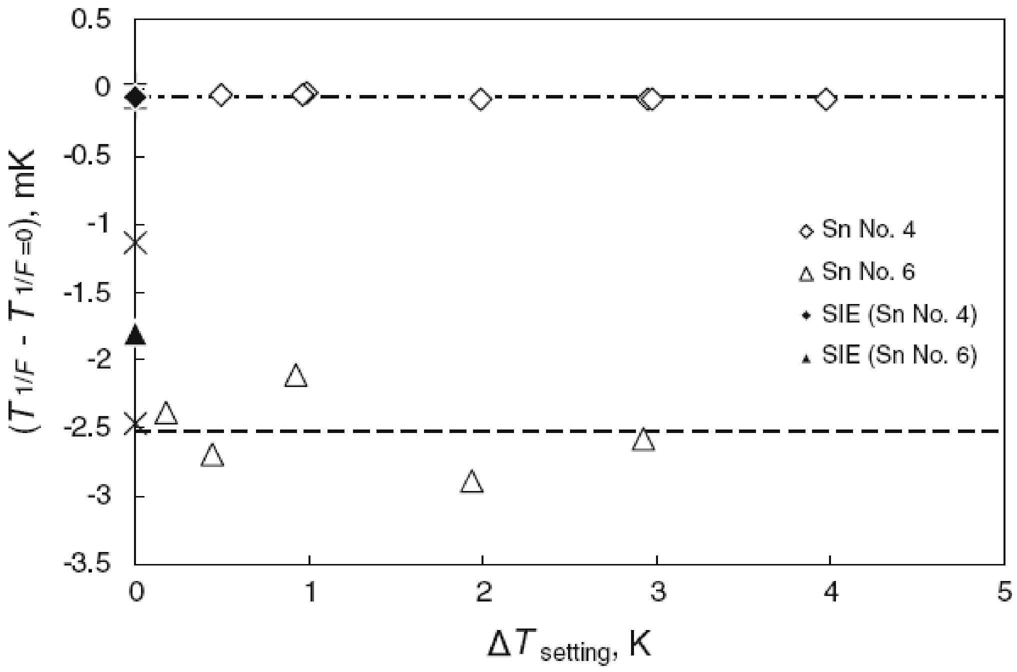

Figure 6 Comparison between the SIE and the slope of the freezing curve obtained from experimental results for Sn cells [5]. The DT_{SIE} and its uncertainty is indicated as the bold plots, and the experimental results are shown in the open plots. The dotted lines show the trend for the slope of the freezing curve against the temperature setting, which is negligibly small.

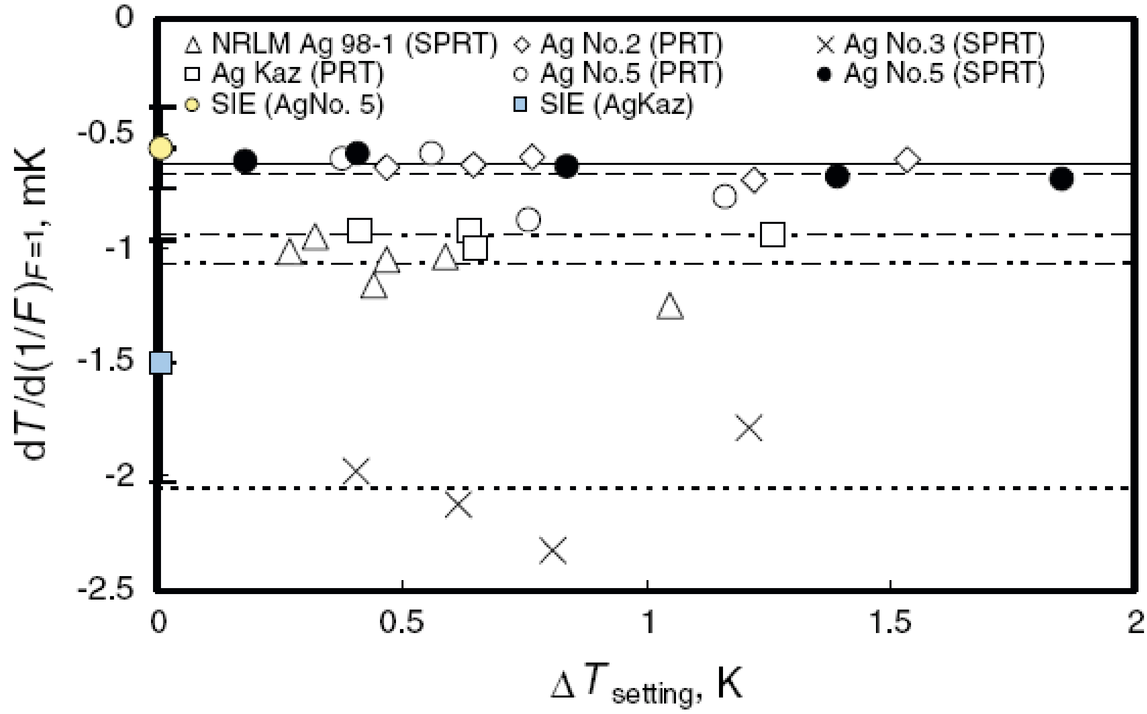

Figure 7 Comparison between the SIE and the slope of the freezing curve obtained from experimental results for Ag cells [6]. The DT_{SIE} and its uncertainty is indicated as the bold plots, and the experimental results are shown in the open plots. The dotted lines show the trend for the slope of the freezing curve against the temperature setting, which is negligibly small.

1.5. Comparison with the direct cell comparison

Direct comparison between different fixed point cells is another method to check the validity of the evaluation method. Table 1 is an example of such an evaluation at the Al point [4]. We can see that the results agree well.

There exists some cases that SIE and the slope of the freezing curve didn't agree with each other, for example as Sn cell No. 6 shown in figure 8. Even in this case, the results of the direct comparison well agreed with the slope of the freezing curve.

Upon these facts upon our cells, we believe that when the fraction of the molten metal F is accurately determined, by methods such as monitoring the heater power fluctuation, the slope of the freezing curve yielded from this determination does have a more reliable figure than as generally recognized as merely a validation method. However, it is doubtless that without having the confidence of the accurate determination of $1/F$, the application thermal analysis would degrade to merely providing some reference information

Furthermore, as figure 8 shows an example, merely relying upon the SIE might cause some misleading conclusions. Verification of the results employing various methods is important.

Table 1 Example of cell comparisons: from direct measurements and from freezing curve evaluation at Al fixed point [4].

	Cell comparison		Thermal analysis	
Cell pair	$\Delta T_{\mathrm{cell,exp}}$/mK	$u_{\mathrm{cell,exp}}$/mK	$\Delta T_{\mathrm{cell,grad}}$/mK	$\Delta T_{\mathrm{cell,grad}} - \Delta T_{\mathrm{cell,exp}}$/mK
Al No 4–NRLM Al 97-1	0.73	0.1	0.70	−0.03
Al No 5–NRLM Al 97-1	0.89	0.07	0.95	0.06
Al No 6–NRLM Al 97-1	1.46	0.04	1.41	−0.05
Al No 5–Al No 4	0.20	0.13	0.24	0.04

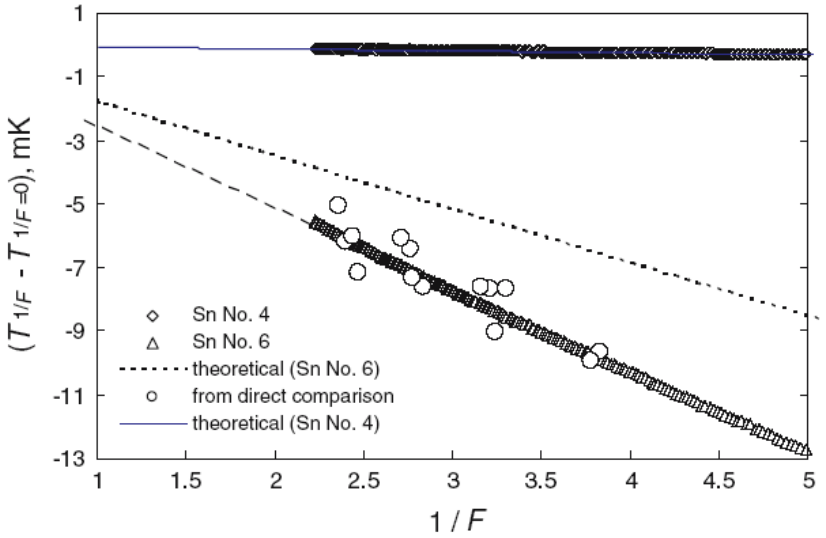

Figure 8 Comparison between the direct comparison (circle plots), the measured freezing curve, and the theoretically calculated freezing curve based upon the pre-fabrication chemical analysis [5]. Cell Sn-6 is one example that theoretical calculations upon SIE does not coincide with the experimental results. However, the results of the two independent experimental methods, freezing curve analysis and direct comparison with other cells, have well agreed.

2. Difficulties in applying the SIE

The SIE and the theoretical prediction of the temperature bias based on the chemical analysis does give us abundant information of the effects caused by the impurities in the metal ingot. We also believe that it would be an almighty method if all the problems are solved to apply it. However, from our experience in producing the fixed-point cells in-house and evaluating them, we have the following concerns as the difficulties in applying the SIE. We expect to play some role to solve these problems in the future work at NMIJ.

2.1 Uncertainty of the chemical analyses and pre/post fabrication analyses

As figure 8 shows, there is always a risk of cell contamination during the fabrication or during the operation of the fixed-point cells. In this concern, we have been exploring the adequate method to have both the pre- and post-fabrication chemical analyses results. Table 2 shows an example of such data for a silver cell. Within the table, cell Ag No. 5 has the pre-fabrication chemical analysis (in the third column, by ICPMS) and post-fabrication (fourth column, by GDMS). Obvious differences have been observed. The impurity Mg has not been detected in the post-fabrication. In contrast, Fe has obviously increased in the post-fabrication analysis. There might be some ambiguity between the results, since the analysis method differs between the pre- and post-fabrication. However, the difference occurred at a level well over the detection limit of the analysis. Since Mg has a higher vapor pressure for temperatures at the silver melting point, we assume that Mg has disappeared due to volatilities.

2.2. Data for the slope of the liquidus line

As already recognized by the CCT-WG1, the data for the basis of the SIE method might have less reliability than the field of thermometry expects. We have had many discussions with our metal supplier, however, they state that some difficulties arise when producing specimens having impurities doped. One of the difficulties is the vapor pressure of the impurity material. Since the impurity might vaporize, the mass of the ingredients upon producing doped metals have less reliability in concerns of impurity concentration.

2.3. Impurities from the graphite crucible

Another problem merely discussed is the impurities generation from the graphite crucible. We currently have no data upon this issue. However we have a large concern upon this.

Table 2 Impurities in the silver fixed-point cells ⁶⁾. Cell Ag No.5 has two results; the third column labeled a) is pre-fabrication, and b) is for post-fabrication.

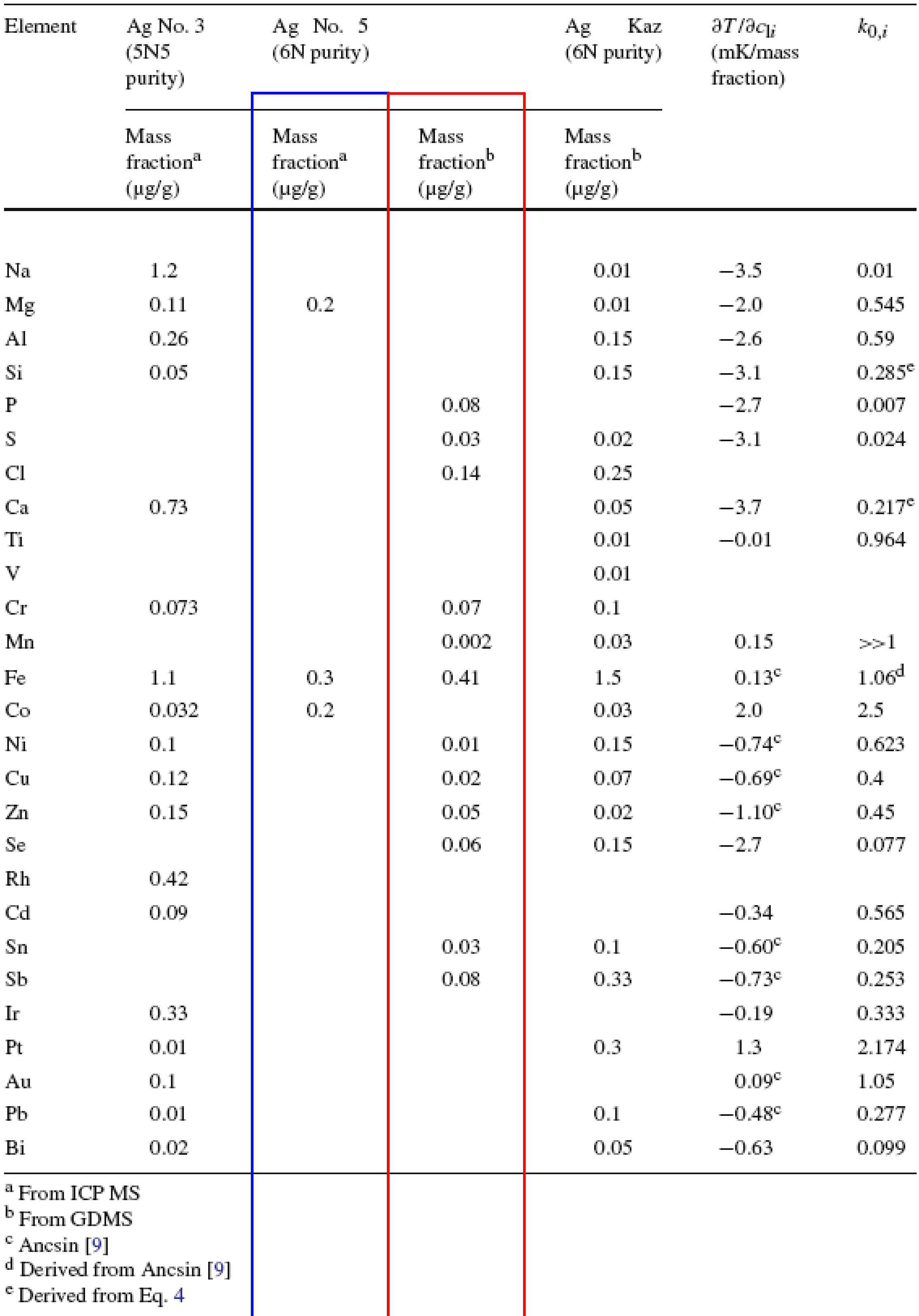

Element	Ag No. 3 (5N5 purity)	Ag No. 5 (6N purity)		Ag Kaz (6N purity)	$\partial T/\partial c_{li}$ (mK/mass fraction)	$k_{0,i}$
	Mass fraction[a] (μg/g)	Mass fraction[a] (μg/g)	Mass fraction[b] (μg/g)	Mass fraction[b] (μg/g)		
Na	1.2			0.01	−3.5	0.01
Mg	0.11	0.2		0.01	−2.0	0.545
Al	0.26			0.15	−2.6	0.59
Si	0.05			0.15	−3.1	0.285[e]
P			0.08		−2.7	0.007
S			0.03	0.02	−3.1	0.024
Cl			0.14	0.25		
Ca	0.73			0.05	−3.7	0.217[e]
Ti				0.01	−0.01	0.964
V				0.01		
Cr	0.073		0.07	0.1		
Mn			0.002	0.03	0.15	>>1
Fe	1.1	0.3	0.41	1.5	0.13[c]	1.06[d]
Co	0.032	0.2		0.03	2.0	2.5
Ni	0.1		0.01	0.15	−0.74[c]	0.623
Cu	0.12		0.02	0.07	−0.69[c]	0.4
Zn	0.15		0.05	0.02	−1.10[c]	0.45
Se			0.06	0.15	−2.7	0.077
Rh	0.42					
Cd	0.09				−0.34	0.565
Sn			0.03	0.1	−0.60[c]	0.205
Sb			0.08	0.33	−0.73[c]	0.253
Ir	0.33				−0.19	0.333
Pt	0.01			0.3	1.3	2.174
Au	0.1				0.09[c]	1.05
Pb	0.01			0.1	−0.48[c]	0.277
Bi	0.02			0.05	−0.63	0.099

[a] From ICP MS
[b] From GDMS
[c] Ancsin [9]
[d] Derived from Ancsin [9]
[e] Derived from Eq. 4

Pre-Fabrication

Post-Fabrication

3. Discussions and Conclusions

From our recent work upon the effect of impurities within the fixed-point cells, we believe that when the fraction of the molten metal F is accurately determined, by methods such as monitoring the heater power fluctuation, the slope of the freezing curve yielded from this determination does have a more reliable figure than as generally recognized as merely a validation method. The SIE and the theoretical prediction of the temperature bias based on the chemical analysis might show abundant information compared to the method relying upon experimental data of the freezing curves. However, in some cases, such as figure 8 might show, merely relying on the SIE might have some limitations. It is also becoming to be recognized that the data for the found of the SIE might be not accurate enough for the field of thermometry is expecting.

NMIJ will continue our activity in producing new cells with pre/ post fabrication chemical analysis and continue to compare the results of the freezing curves obtained from our evaluation method of the $1/F$, and expect to play some role to solve the problems related to the application of the SIE through our future work at NMIJ.

Intrinsically, the results of the SIE and the thermal analysis should coincide. However, we should be well aware on those drawbacks of the both methods in applying these methods to our evaluation of the fixed-point temperature in our realization.

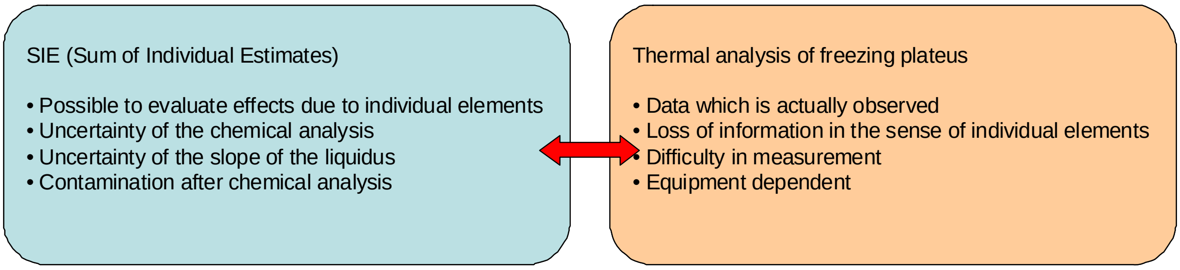

Figure 9 Limits of the SIE and the thermal analysis of the freezing plateaus

References

1. D. Ripple, B. Fellmuth, M. de Groot, Y. Hermier, K. D. Hill, P. P. M. Steur, A. Pokhodun, M. Matveyev, P. Bloembergen P, *CCT Document* **CCT/05-08** (2005).
2. B. Fellmuth, K. D. Hill *Metrologia* **43**:71 (2006).
3. Widiatmo J V, Harada K and Arai M, Trans. SICE **42** 115–22 (2006).
4. J. V. Widiatmo, K. Harada, K. Yamazawa, M. Arai, *Metrologia* **43**:561 (2006).
5. K. Yamazawa, J. V. Widiatmo, M. Arai, *Int. J. Thermophys.* **28**: 1941 (2007).
6. J. V. Widiatmo, K. Harada, K. Yamazawa, M. Arai, *Int. J. Thermophys.* **29**: 158 (2008).